Streamer-induced transport in electron temperature gradient turbulence

T. Hauff and F. Jenko
Max-Planck-Institut für Plasmaphysik, EURATOM Association, 85748 Garching, Germany

(Received 17 July 2009; accepted 18 September 2009; published online 15 October 2009)

The question if and how streamers (i.e., radially elongated vortices) can lead to an enhancement of the electron heat transport in electron temperature gradient turbulence is addressed. To this aim, the electrons are treated as passive tracers, and their decorrelation mechanisms with respect to the advecting electrostatic potential are studied. A substantial transport enhancement is found in a wide region of parameter space. © *2009 American Institute of Physics*. [doi:10.1063/1.3245163]

I. INTRODUCTION

It is well known by now that microturbulence in toroidal magnetized plasmas often tends to form anisotropic structures such as zonal flows or streamers. The former are the $E\times B$ flows resulting from purely radial variations of the electrostatic potential (for a review, see Ref. 1), whereas the latter are radially elongated vortices, generally localized at the outboard side and pointing away from the torus axis (see, e.g., Refs. 2–4). Due to their fundamentally different character, a coexistence of both types of structures can be excluded; rather, one (or none) of them will dominate. However, in both cases, it can be expected that the presence of the structures may have a significant impact on the resulting turbulent transport. While in the case of zonal flows, it is widely accepted that the cross-field transport is reduced or even quenched (see, e.g., Ref. 5), there are only few dedicated investigations concerning the streamer case. It is thus the main goal of the present paper to address the key issue in this context, namely, to which degree and in which way will the presence of streamers enhance the radial turbulent transport? To this aim, we will systematically study the behavior of passive tracers advected in turbulent electrostatic potentials exhibiting streamers.

This question was raised, in particular, by gyrokinetic simulations which showed that the transport levels in electron temperature gradient (ETG) turbulence can clearly exceed naive mixing length expectations, $\chi_e \gg \rho_e^2 v_e/L_{T_e}$.[4,6,7] Here, χ_e is the electron heat diffusivity, ρ_e is the electron thermal gyroradius, v_e is the electron thermal velocity, and L_{T_e} is a characteristic scale length of the electron temperature profile. For cyclone base case parameters,[8] neglecting magnetic electron trapping as well as kinetic ion effects, $\chi_e > 10\rho_e^2 v_e/L_{T_e}$ was obtained in these studies. More recently, taking magnetic trapping into account, it was found that the simulations can reach very high transport levels, generally even failing to saturate (see, e.g., Refs. 9–11). Therefore, in the context of a careful comparison between five different gyrokinetic codes, the magnetic shear value was reduced from 0.8 to 0.1 in order to circumvent these problems.[12,13] Here, it was found that $\chi_e > 5\rho_e^2 v_e/L_{T_e}$ in well-resolved runs for a given box size, and all codes agreed with each other within fairly narrow margins. Finally, recent gyrokinetic simulations including both ion and electron space-time scales self-consistently (but working with a reduced ion-to-electron mass ratio of 400) confirmed these findings in the framework of a more complete and realistic physical setting.[14] In particular, if ion temperature gradient modes are sufficiently close to marginality (as they will be in any experiment) or even stable (as they are in certain dedicated experiments with strong electron heating), one again finds $\chi_e \gg \rho_e^2 v_e/L_{T_e}$. The common feature in all of these simulations is the existence of streamers and relatively weak zonal flow activity. (We note in passing that another such example is trapped electron mode turbulence in the cold ion regime.[15,16])

On general grounds, it is reasonable to expect an enhancement of the turbulent transport in the presence of streamers. First, the very existence of streamers is an indicator of the relative weakness of zonal flows, thus allowing for potentially larger fluxes. Second, according to the common notion that in the saturated state, the radial gradients of the background temperature and the temperature fluctuations should be similar (on average), the amplitude of radially elongated streamers should exceed those of isotropic vortices with the same poloidal extension, increasing the resulting transport level. Third, even if the amplitude of the vortices is kept constant, a radial elongation can raise the cross-field diffusivity due to the larger radial correlation length. The latter effect shall be investigated in more detail in the present paper, establishing a closer link between turbulent structures and corresponding transport levels. To this aim, we will employ a passive tracer description (like in Refs. 17 and 18) which allows for a simpler, more accessible, and more rigorous treatment of the questions under consideration.

To avoid misunderstandings, it should be pointed out in this context that the passive tracer diffusivity D and the self-consistent particle diffusivity $D_s=-\Gamma/\nabla n$ (where $\Gamma=\langle\tilde{n}\tilde{v}\rangle$ is the fluctuation-induced particle flux) are two very distinct quantities. Whereas the latter is zero in the adiabatic-ion approximation and, in general, still close to zero in a kinetic description, the former reflects the mixing properties or the "self-diffusion" of a turbulent flow, thus having a finite value. However, it is possible to establish a connection between D and the electron heat flux Q. In Ref. 19, for instance, it was shown numerically that the test particle heat flux $Q=-\int(mv^2/2)D(v)\,\partial f_0/\partial r d^3v$ is very close to its self-consistent counterpart $Q_s=\int(mv^2/2)\tilde{v}_{E\times B}\tilde{f}d^3v$. Setting $f_0 \propto n_0 T_0^{-3/2} e^{-mv^2/2T_0}$ and ignoring the density gradient, we obtain $Q=\int mv^2/2T_0(mv^2/2T_0-3/2)D(v)f_0 d^3v\,\partial T_0/\partial r$ for the

heat flux. From this, one gets $\chi \sim D$ for the (electron) heat conductivity. Thus, test particle transport as discussed in this paper is not only relevant for describing the mixing properties of passive tracers, but it is directly related to the more important question of heat transport.

The remainder of this paper is organized as follows. In Sec. II, a brief review of pure drift orbit center motion in anisotropic turbulence is given. In Sec. III, a validity condition for orbit averaging is introduced and its impact on the transport of suprathermal particles is reviewed. In Sec. IV, the diffusive motion of thermal test particles is studied in detail, and the consequences of the invalidity of drift orbit averaging for the decorrelation mechanisms of these particles are examined by means of a simplified model. In Sec. V, the scaling of the diffusion coefficient with the turbulence amplitude and correlation length is studied for ETG turbulence. Finally, in Sec. VI we provide a summary along with some conclusions.

II. TRANSPORT SCALING FOR PARTICLE ORBIT CENTERS

In a first step, we will take a look at some basic properties of particle drift orbits in axisymmetric toroidal systems. As is well known, while basically following the magnetic field lines, a particle in a tokamak undergoes both a gyromotion as well as a drift orbit motion (induced by curvature and grad-B drifts) perpendicular to the magnetic field. In a field-aligned coordinate system, the latter corresponds to an approximately circular (actually slightly elliptical) trajectory in the perpendicular plane.[17] Provided that gyroaveraging and drift orbit averaging are both valid, the turbulent motion of passive particles in prescribed electrostatic fluctuations can thus be well described by the $E \times B$ drift in a gyro/orbit averaged potential.

For now, we would like to restrict to pure $E \times B$ motion in two dimensions, various generalizations will follow later. In an isotropic electrostatic potential, the scaling of the diffusion coefficient $D_i(t) \equiv 1/2d/dt\langle[x_i(t)-x_i(0)]^2\rangle$ with the characteristic values of the turbulent electrostatic potential is well known. In terms of the correlation length λ_c, the correlation time τ_c, and the average $E \times B$ velocity V (which corresponds to the fluctuation amplitude), the scaling of D_i can be expressed as[20–22]

$$D_i \propto \lambda_c^{2-\gamma} V^{\gamma} \tau_c^{\gamma-1}. \tag{1}$$

Here, the exponent γ strongly depends on the strength of (electrostatic) trapping, which is measured by the Kubo number[22] $K \equiv \tau_c/\tau_{\mathrm{fl}} \equiv \tau_c V/\lambda_c$. For $K \ll 1$ (linear or ballistic regime), simple considerations lead to $\gamma=2$, whereas for $K \gg 1$ (nonlinear regime) one finds $\gamma=0.7$.[23,24] Moreover, for $K \approx 1$, $\gamma \approx 1$. As can be inferred from Eq. (1), for fixed V and λ_c, the spatial structure of a turbulent field is only relevant for $\gamma<2$, i.e., for $K \gtrsim 1$.

In Ref. 25, it was shown that anisotropic structures (like streamers) can be described in a similar way by using λ_x and V_x for the diffusivity in the x direction and λ_y and V_y for the diffusivity in the y direction in Eq. (1). Defining an anisotropy factor $\zeta \equiv \lambda_x/\lambda_I$ (the index I denotes the isotropic value), one therefore finds $D_x \propto \zeta^{2-\gamma}$ if λ_y is kept unchanged. This means that in the large Kubo number regime, anisotropic structures enhance the tracer transport. Since realistic Kubo numbers are found (in nonlinear gyrokinetic simulations) to lie between about 1 and 10 (corresponding to γ values somewhere between 0.7 and 1), this effect is relevant if no faster decorrelation mechanism exists.

In Ref. 25 the influence of a homogeneous background drift of the turbulence on the transport was also a subject of study. It was shown that a potential drift with velocity v_{dr} in the y direction leads to a strong suppression of transport at a characteristic "drop time" $\tau_{\mathrm{drop}} \equiv 2\lambda_y/v_{\mathrm{dr}}$. This effect is important for $\tau_{\mathrm{drop}} \lesssim \tau_c$, whereas it has no influence for $\tau_{\mathrm{drop}} \gg \tau_c$. Typically, one finds $\tau_{\mathrm{fl}} < \tau_{\mathrm{drop}} \lesssim \tau_c$, which implies only a moderate decrease in the diffusion coefficient compared to a nondrifting case.

In the preceding discussion, the only relevant decorrelation mechanism was the time dependence of the electrostatic potential. However, decorrelation may also be caused by the parallel motion of the particle along the magnetic field lines or, if drift orbit averaging is not valid, by the orbit motion perpendicular to the magnetic field lines. If we denote the respective effective decorrelation time by τ^{eff}, and one has $\tau^{\mathrm{eff}} < \tau_c$, τ_c is to be replaced by τ^{eff} in the preceding discussion to obtain the correct scaling behavior of the diffusion coefficient. For clarification, we would like to mention that in the present paper, the term "(drift) orbit motion" refers to the curvature and grad-B drift motion and does not include the gyromotion, which is on a much faster time scale than the particle drifts, and therefore not an origin of decorrelation.

III. TRANSPORT SCALING FOR SUPRATHERMAL PARTICLES

Next, we would like to discuss what happens if the orbit averaging procedure is not valid, i.e., if the particle motion cannot be explained by the (effective) $E \times B$ drift alone. As pointed out in Ref. 17, a criterion for the validity of orbit averaging is that the particle displacement after one drift orbit turn is smaller than a correlation length. Since the displacement may be caused by the $E \times B$ drift as well as by the particle or turbulence toroidal drift, the condition for the validity of orbit averaging can be expressed as

$$\Xi_{\mathrm{o.a.}} \equiv \max\{V, |v_{\mathrm{dr}} - v_y|\} \frac{T_{\mathrm{orbit}}}{\lambda_c} \lesssim 1, \quad T_{\mathrm{orbit}} \ll \tau_c, \tag{2}$$

T_{orbit} being the orbit circulation time, v_{dr} the background toroidal drift of the fluctuations, and v_y the particle toroidal (precession) drift. In Ref. 17, it was shown that one typically finds $\Xi_{\mathrm{o.a.}} > 1$, i.e., orbit averaging is not valid in general. Following this finding, energetic particles with $E \gg T_{i,e}$ were discussed. Their drift orbit diameter Δr is much larger than the correlation length of the potential, for both trapped and passing particles. Therefore the particle decorrelates already after a time,

$$\tau^{\mathrm{orbit}} = \lambda_c/v_{\mathrm{orbit}} = \lambda_c T_{\mathrm{orbit}}/(\pi \Delta r). \tag{3}$$

Since $\tau^{\text{orbit}} \equiv \tau^{\text{eff}} < \tau_{\text{fl}}$, the particles are in the ballistic regime when they decorrelate, and the diffusion coefficient can therefore be approximated by $D \approx V^2 \tau^{\text{orbit}} \propto V^2 \lambda_c$. This expression cannot be associated with an exponent γ in the context of Eq. (1). Moreover, although the transport in that regime depends on the turbulence correlation length λ_c, it is not affected by structural anisotropies because the particles do not follow equipotential lines. Instead, they decorrelate due to the drift orbit motion, which is governed by the smallest correlation length. For radial streamers, this means that only λ_y contributes to D, but not λ_x. Furthermore, it was found that for suprathermal particles, the orbit decorrelation time is smaller than the parallel one ($\tau^{\text{orbit}} < \tau_{\parallel}$). Hence, the parallel motion was ignorable. In the following sections, we will study to which degree the findings for energetic particles on one hand and for pure $E \times B$ motion in two dimensions on the other hand carry over to thermal particles in a tokamak, namely, electrons in ETG turbulence.

IV. BASIC STUDIES OF THERMAL PARTICLES IN ETG-LIKE TURBULENCE

In order to get an idea of a reasonable choice of various quantities mentioned above, we have performed nonlinear gyrokinetic simulations (in the local limit) of ETG turbulence with kinetic ions for cyclone base caselike parameters,[8] employing the GENE code.[4,15] The simulations have been performed in $\hat{s}-\alpha$ geometry, with $\alpha=0$, $\hat{s}=0.8$, $r/R=0.18$, $q=1.4$, $T_e=T_i$, and $n_e=n_i$. We have used a reduced mass ratio $m_i/m_e=400$, and have taken $R/L_n=2.22$ and $R/L_{T_e}=R/L_{T_i}=6.92$ for the gradients. The perpendicular box size was chosen to be $(L_x, L_y)=(250.0\rho_e, 128.0\rho_e)$, and we have used $128\times128\times16$ grid points in the radial, binormal, and parallel directions, respectively, as well as 32×8 grid points in $(v_{\parallel}, \mu)$ space, with box sizes of $(L_v, L_\mu)=(3,9)$. This way, we found

$$\begin{aligned}
&\sqrt{\langle \phi^2 \rangle} \approx 60(\rho_e/R)(T_e/e), \quad \tau_c \approx 12R/v_e, \\
&\lambda_x \approx 23\rho_e, \quad \lambda_y \approx 7.0\rho_e, \\
&V_{x,0} \approx 12\rho_e v_e/R, \quad V_{y,0} \approx 7.5\rho_e v_e/R, \\
&v_{\text{dr}} \approx 2.2\rho_e v_e/R, \quad \tau_{\text{drop}} \approx 6.4R/v_e, \\
&\tau_{\text{fl},x} \approx 1.8R/v_e, \quad K_x \approx 7.
\end{aligned} \tag{4}$$

Here, R is the major radius, and the other quantities have already been defined above. These numbers are in good agreement with those obtained in the framework of recent benchmarking simulations.[12] Thus, they seem to represent rather typical values for the above quantities. (In global adiabatic-ion simulations of ETG turbulence,[18] much larger correlation lengths and times have been observed, but the difficulties of using the adiabatic-ion approximation in the presence of trapped electrons mentioned in Sec. I make their interpretation hard.) Nevertheless, in the following discussions, we do not want to restrict to those values. Instead, we will study the transport of thermal electrons in ETG turbulence under rather general conditions. This procedure seems to be adequate since we will see that the transport behavior may depend on the interplay of various different time scales in a very sensitive way, rendering it impossible to claim that the transport scaling of a particular realization of ETG turbulence applies universally. In this context, we would like to note that we have used the e-folding length or time to determine the correlation parameters, since our practical experience shows that this procedure yields the most reliable results. The circulation time and orbit diameter of a thermal electron can be calculated to be[26] $T_{\text{orbit}}=2\pi qR/v_e \approx 9R/v_e$ and $\Delta r=2q\rho_e \approx 2.8\rho_e$, respectively, with q being the safety factor.

To gain a basic understanding of the electron dynamics under such conditions, we simulate the drift orbit motion of the particles relative to the field aligned coordinates by a simple two-dimensional (2D) model defined by

$$\dot{\mathbf{x}} = \mathbf{v} - \nabla\phi \times \mathbf{e}_z, \quad \dot{\mathbf{v}} = \omega_{\text{orbit}} \mathbf{v} \times \mathbf{e}_z. \tag{5}$$

Equation (5) describes a particle which is forced on a circular orbit with $\omega_{\text{orbit}}=2\pi/T_{\text{orbit}}$, at the same time undergoing an $E \times B$ drift motion. The orbit radius is set by choosing an appropriate initial velocity of the particle. This model is very useful for general studies, since all orbit parameters can be varied independently, and the real drift orbit in field aligned coordinates is fitted well. Its validity has been demonstrated via direct comparisons with simulations in tokamak geometry.[17] Of course, no parallel decorrelation effects can be observed with this model. We will include them later.

Using Eq. (2), one obtains $\Xi_{\text{o.a.}} \approx 5$, which means that drift orbit averaging is not valid. Additionally, $T_{\text{orbit}} \approx \tau_c$. So on one hand, the thermal electrons will not follow the equipotential lines of the (orbit averaged) vortex structures strictly. On the other hand, since $\Delta r \ll \lambda_{x,y}$, the particle is not able to significantly depart from its initial equipotential line and decorrelate during one orbit turn. What we therefore expect to happen is that the particle at least roughly follows the turbulent structures, deviating, in particular, at certain positions, e.g., at a saddle point, or at a point where the equipotential line exhibits a sharp bend.

In Fig. 1, an electrostatic potential with the scales of Eq. (4) is plotted together with trajectories of particles with thermal velocity. The drift in the y direction is kept, but the fluctuations are frozen for the purpose of a better demonstration of the interaction effects. Both the potential and the trajectories have been transformed into the comoving frame. As pointed out in Ref. 25, the potential in that frame is given by

$$\phi'_{\text{dr}}(x,y,t) = \phi_{\text{dr}}(x, y + v_{\text{dr}}t) - v_{\text{dr}}x, \tag{6}$$

which is a superposition of the stochastic part without y drift and a static ramp in the x direction, which acts as a transport barrier. In Fig. 1, a pure $E \times B$ drift trajectory without any 2D orbit effects is compared with the trajectory of a thermal particle, which undergoes both $E \times B$ drift and orbit motion. As we have expected, this particle roughly follows the lines of the stream function due to its small orbit diameter. However, we see that at a point where neighboring lines diverge

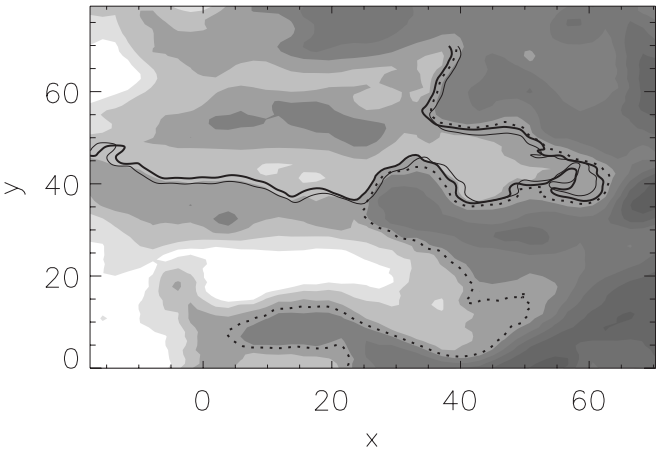

FIG. 1. ETG-type electrostatic potential with drift in the y direction and particle trajectories, transformed into the comoving frame (field aligned coordinates). Dashed line: pure $E\times B$ drift without drift orbit effects. Solid line: $E\times B$ drift with particle orbit motion (bold line: particle trajectory; thin line: orbit center). The deviation from the equipotential lines at a saddle point can be observed.

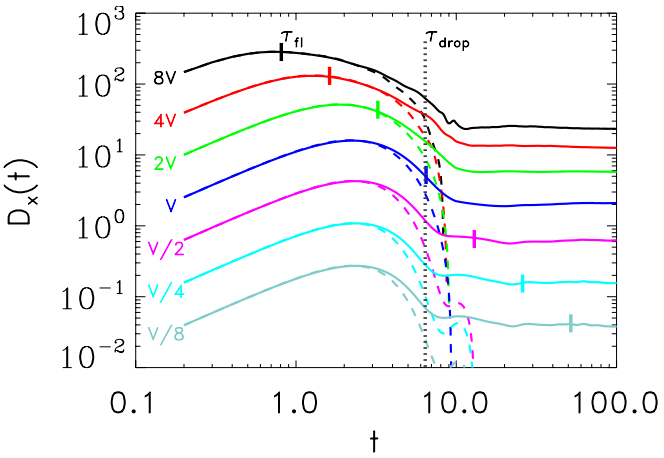

FIG. 2. (Color online) Running diffusion coefficient in an artificially created, ETG-like electrostatic potential. For the nominal amplitude V, $\tau_{fl} \equiv \tau_{drop}$. V is then varied according to the values plotted left of the curves. Dashed line: pure $E\times B$ drift. Solid line: $E\times B$ drift with 2D orbit effects.

(this seem to be saddle points coinciding with a sharp bend), the oscillating trajectory diverges from the nonoscillating one. This, in turn, means that the drift orbit motion of a particle weakens the barrier caused by the background drift of the potential, and defines a time scale on which the transport becomes diffusive, since the departure from the equipotential lines can be interpreted as a random process.

What is the time scale of that random process? It depends on the typical time between two random departures from the equipotential line. The distance between two of these points (saddle points or points of large curvature of the stream function) can be approximated by the extension of the structures of the potential in the comoving frame. As can be seen in Fig. 1 (and was pointed out in Ref. 25), there are dominant structures on two scales in the x direction. The first scale is given by the correlation length λ_x (closed equipotential lines in Fig. 1), whereas the second scale is given by the maximal extent of the open contours in the x direction, which is $x_{max}=2V_x\lambda_y/v_{dr}$.[25] In Fig. 1, we have $\lambda_x\approx 23$ and $x_{max}\approx 80$. The respective time scales are $\lambda_x/V_x=\tau_{fl}$ and $x_{max}/V_x=\tau_{drop}$. For a potential with a significant drift velocity v_{dr}, the open equipotential lines are dominating the closed vortices in the comoving frame. Therefore we will find that the larger scales, x_{max} or τ_{drop}, on the spatial or temporal scale, respectively, are dominating the decorrelation process. Here, we would like to note that while the curve in Fig. 1 has been chosen to illustrate our argument, the latter can be shown to be generally applicable.

In order to do that, we put a sufficiently large number of test particles into an artificially created electrostatic potential and calculate the diffusion coefficient for both the 2D orbit model of Eq. (5) as well as a pure $E\times B$ drift motion without any orbit effects. The electrostatic potential is created as a superposition of 10^3 plane waves,[25,27] and its scales correspond to the ones of Eq. (4)—with two exceptions: the turbulence is frozen (but the y drift is kept) and the amplitude is reduced by a factor of 3.6. The former change is done in order to ignore temporal decorrelation effects for the moment, whereas the latter is done to enforce $\tau_{fl}=\tau_{drop}$. Moreover, no parallel dynamics effects are included.

The result is plotted in Fig. 2. Here, V is varied, and the actual value of τ_{fl} is indicated. We see that for the pure $E\times B$ motion, the diffusivity drops to zero at $t\sim\tau_{drop}$ for all amplitudes, since there is no decorrelation mechanism which would allow the particles to cross the barrier produced by the y drift (remember that we have switched the time dependence of the fluctuations off). For the particles on the 2D drift orbit, however, we observe that they decorrelate at $t\sim\tau_{drop}$, which leads to the saturation of the diffusion coefficient. So in that case, τ_{drop} resumes the role of τ^{eff}, and we can assume that for $\tau_{fl}\gg\tau_{drop}$ we will find $D\propto V^2(\gamma=2)$, whereas for $\tau_{fl}\ll\tau_{drop}$, we will find $D\propto V^{0.7}(\gamma=0.7)$, which will correspond to an effective low or high Kubo number regime, respectively. From Fig. 2, we obtain $\gamma=2$ for $\tau_{fl}\gg\tau_{drop}$ and $\gamma\approx 0.85$ for $\tau_{fl}\ll\tau_{drop}$. This result confirms the claims we have made at the beginning of this section.

Finally, we would like to emphasize one important point. If a V^2 dependence of the transport is observed (ballistic regime), this does not necessarily mean that the particles decorrelate due to the temporal decorrelation of the fluctuations, or due to the parallel motion with a decorrelation time $\tau_\parallel\ll\tau_{fl}$. The perpendicular decorrelation at τ_{drop}, caused by deviations from the equipotential lines due to finite drift orbit effects at hyperbolic fix points, is able to induce the same behavior. Therefore, decorrelation will occur at $\tau^{eff}=\min\{\tau_{drop},\tau_\parallel\}$. In Sec. V, we will examine which decorrelation time is the smaller, i.e., dominating, one.

V. THERMAL PARTICLES IN GYROKINETIC ETG TURBULENCE

We now return to the gyrokinetic ETG turbulence simulated with GENE, characterized by the parameters of Eq. (4). In order to obtain the values of the electrostatic potential between grid points, the original data are interpolated via spectral methods, which provide the highest possible spatial

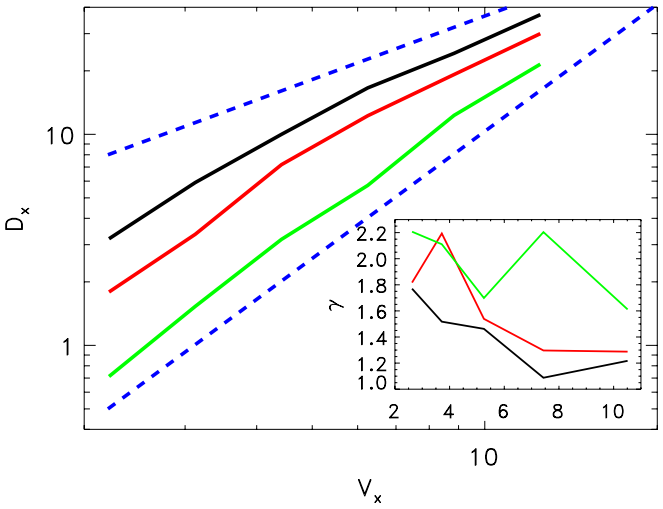

FIG. 3. (Color online) Saturated diffusion coefficient in a gyrokinetic ETG potential, with V reduced artificially starting from the original value of $V_x = 12.5\rho_e v_e/R$. Dark (black) line: no parallel decorrelation. Dark gray (red) line: mimicked parallel correlation length $\lambda_\parallel = 1.6\pi qR$ using $\tau_c = 7.0R/v_e$. Light gray (green) line: mimicked parallel correlation length $\lambda_\parallel = 0.8\pi qR$ using $\tau_c = 3.5R/v_e$. Inset: scaling exponent γ vs V.

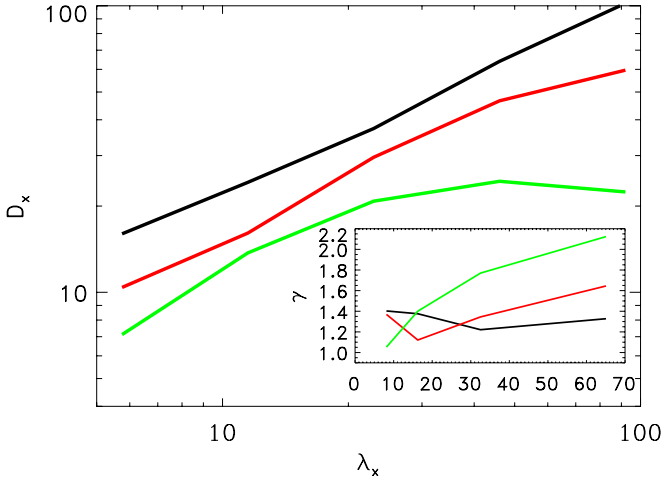

FIG. 4. (Color online) Same as previous figure, but λ_x is varied instead of V_x, starting from the original value of $\lambda_x = 23\rho_e$.

accuracy. The differential Eq. (5) is solved via a fourth-order Runge–Kutta algorithm. In order to obtain the scalings of the diffusion coefficient with V_x and λ_x, the original values are modified. In Sec. IV, we have discussed the consequences of a decorrelation at τ_{drop}, whereas we have ignored possible decorrelation effects due to the parallel motion of the thermal particles. While for very energetic particles, it could be shown that decorrelation due to the perpendicular motion is much faster than due to the parallel one,[17] this is not necessarily the case for thermal particles. This is due to their smaller orbit diameter ($\Delta r < \lambda_c$), which does not bring them out of the correlated zone on a time scale smaller than the orbit time.

The time scales which can be inferred from Eq. (4) (and which are close to the values presented in Ref. 12), imply that $\tau_{\text{drop}} \approx 6.4R/v_e$, whereas an orbit time for passing particles with a pitch angle of unity can be calculated to be $T_{\text{orbit}} = 2\pi qR/v_e \approx 8.8R/v_e$. Our ETG simulations exhibit $\lambda_\parallel \approx 0.8\pi qR$, meaning that $\tau_\parallel \approx 3.5R/v_e$, which is smaller than τ_{drop} and therefore dominates the decorrelation process.

We mimic the effect of parallel decorrelation by artificially reducing the correlation time of the fluctuations. For example, for passing particles, a reduction to $\tau_c = 3.5R/v_e$ has the same effect than a decorrelation due to the finite parallel extension of the turbulent structures with $\lambda_\parallel = 0.8\pi qR$. This is allowed since for the transition from the initial ballistic regime to a later diffusive regime, it is irrelevant if the decorrelation is temporal or spatial. We have to keep in mind, though, that only the passing particles with large pitch angles are subject to this parallel decorrelation, whereas for trapped particles, the decorrelation comes from temporal or perpendicular effects. Figure 3 shows the saturated diffusion coefficient for a number of different mean drift velocities V_x. The black curve ignores parallel decorrelation effects, whereas the light gray curve corresponds to a realistic parallel correlation length by reducing τ_c to $3.5R/v_e$. All curves show a decline of diffusivity when the drift velocity is reduced. The black curve shows a scaling exponent γ growing with the reduction of the mean drift velocity, which can be explained by the fact that τ_{fl} gets larger than τ_{drop} for $V_x < 3.6$. This, in turn, means that the effective decorrelation time moves into the ballistic regime. For the light gray curve, the effective decorrelation time is $\tau^{\text{eff}} = \tau_\parallel = 3.5R/v_e$, which is smaller than τ_{drop} and therefore dominating. Hence, the transition to the ballistic regime $\gamma \to 2$ occurs already at larger V_x.

Figure 4 shows the saturated diffusion coefficient for a number of different radial correlation lengths, while $V_{x,0}$ stays constant. Here, we observe a transition to the ballistic regime for large anisotropy (large λ_x), which is stronger for the curves with parallel decorrelation. τ_{fl} increases with growing λ_x, which means that for large λ_x, it exceeds the effective decorrelation time. Since the latter is smaller with parallel decorrelation effects, the transition occurs earlier in that case. A consequence of that behavior is that, for the light gray curve (passing particles with parallel decorrelation) there is no increase in the diffusivity for very large radial correlation lengths.

For the nominal parameters of our ETG simulations with GENE, we find $\gamma \sim 1.2$ for trapped particles (decorrelation at τ_{drop}), and $\gamma \sim 1.6$ for passing particles (decorrelation at $\tau_\parallel$), which is between the ballistic and the vortex trapping regime. This means that the presence of streamers indeed increases the transport of passive tracers. This increase is less than linear in the streamer length, however. Generally, γ is larger for passing particles with parallel decorrelation than for trapped particles, since decorrelation occurs earlier. For both trapped and passing particles, a transition to ballistic transport ($\gamma = 2$) occurs for small turbulence amplitudes or large radial vortex extension. As a rough criterion for ballistic transport, we find $\tau^{\text{eff}} = \min\{\tau_{\text{drop}}, \tau_\parallel\} \ll \tau_{\text{fl}} = \lambda_x/V_x$. This rule of thumb can serve as a first test to find out if a particular turbulence simulation is likely to exhibit streamer-induced transport enhancement or not.

VI. SUMMARY AND CONCLUSIONS

In the present paper, we have addressed the question if and how streamers (i.e., radially elongated vortices) can lead to an enhancement of the cross-field transport of passive tracers. Here, our focus was on the dynamics of thermal electrons in the context of ETG turbulence, although our results may also be applied to other types of streamer-dominated turbulence, driven, e.g., by trapped electron modes.

We have shown that for thermal electrons in ETG turbulence, drift orbit averaging is not valid. Nevertheless, due to its small drift orbit diameter, a particle is not able to decorrelate after one orbit turn and therefore still roughly follows the contour lines of the electrostatic potential. We have seen that decorrelation typically occurs at hyperbolic fixed points, whose typical distance is $x_{\max}=2V_x\lambda_y/v_{\mathrm{dr}}$. This decorrelation scale is dominated by the potential structure in the frame moving with the diamagnetic background drift of the vortices and leads to an effective decorrelation time of $\tau^{\mathrm{eff}}=\tau_{\mathrm{drop}}$. However, the decorrelation due to the finite parallel extension of the turbulent structures is typically on a smaller time scale, leading to a decorrelation at the minimum value of τ_{drop} and $\tau_{\parallel}$.

If this effective decorrelation time is significantly smaller than the vortex turnover time $\tau_{\mathrm{fl}}=\lambda_x/V_x$, the transport is in the ballistic regime, which means that $\gamma=2$ and that the spatial vortex structure has no influence on the transport. This implies that there is an upper limit to the streamer-induced *geometric* transport enhancement, while there still might be an indirect, amplitude-dependent contribution. However, for the nominal turbulence parameters of our simulations (and as well as from other codes), we get $\tau_{\mathrm{fl}}<\tau^{\mathrm{eff}}$, and we find $1<\gamma<2$. Due to the direct relation between test particle diffusion and heat conductivity, this amounts to a significant influence of the spatial vortex structure on the electron heat transport.

ACKNOWLEDGMENTS

We thank T. Görler for providing the simulation data obtained with the GENE code.

[1] P. H. Diamond, S.-I. Itoh, K. Itoh, and T. S. Hahm, Plasma Phys. Controlled Fusion **47**, R35 (2005).
[2] J. F. Drake, P. N. Guzdar, and A. B. Hassam, Phys. Rev. Lett. **61**, 2205 (1988).
[3] S. C. Cowley, R. M. Kulsrud, and R. Sudan, Phys. Fluids B **3**, 2767 (1991).
[4] F. Jenko, W. Dorland, M. Kotschenreuther, and B. N. Rogers, Phys. Plasmas **7**, 1904 (2000).
[5] P. W. Terry, Rev. Mod. Phys. **72**, 109 (2000).
[6] W. Dorland, F. Jenko, M. Kotschenreuther, and B. N. Rogers, Phys. Rev. Lett. **85**, 5579 (2000).
[7] F. Jenko and W. Dorland, Phys. Rev. Lett. **89**, 225001 (2002).
[8] A. M. Dimits, G. Bateman, M. A. Beer, B. I. Cohen, W. Dorland, G. W. Hammett, C. Kim, J. E. Kinsey, M. Kotschenreuther, A. H. Kritz, L. L. Lao, J. Mandrekas, W. M. Nevins, S. E. Parker, A. J. Redd, D. E. Shumaker, R. Sydora, and J. Weiland, Phys. Plasmas **7**, 969 (2000).
[9] Y. Idomura, Phys. Plasmas **13**, 080701 (2006).
[10] A. Bottino, A. G. Peeters, R. Hatzky, S. Jolliet, B. F. McMillan, T. M. Tran, and L. Villard, Phys. Plasmas **14**, 010701 (2007).
[11] J. Candy, R. E. Waltz, M. R. Fahey, and C. Holland, Plasma Phys. Controlled Fusion **49**, 1209 (2007).
[12] W. M. Nevins, J. Candy, S. Cowley, T. Dannert, A. Dimits, W. Dorland, C. Estrada-Mila, G. W. Hammett, F. Jenko, M. J. Pueschel, and D. E. Shumaker, Phys. Plasmas **13**, 122306 (2006).
[13] W. M. Nevins, S. E. Parker, Y. Chen, J. Candy, A. M. Dimits, W. Dorland, G. W. Hammett, and F. Jenko, Phys. Plasmas **14**, 084501 (2007).
[14] T. Görler and F. Jenko, Phys. Rev. Lett. **100**, 185002 (2008).
[15] T. Dannert and F. Jenko, Phys. Plasmas **12**, 072309 (2005).
[16] J. Lang, Y. Chen, and S. E. Parker, Phys. Plasmas **14**, 082315 (2007).
[17] T. Hauff and F. Jenko, Phys. Plasmas **15**, 112307 (2008).
[18] Z. Lin, I. Holod, L. Chen, P. H. Diamond, T. S. Hahm, and S. Ethier, Phys. Rev. Lett. **99**, 265003 (2007).
[19] Z. Lin and T. S. Hahm, Phys. Plasmas **11**, 1099 (2004).
[20] J. H. Reuss and J. D. Misguich, Phys. Rev. E **54**, 1857 (1996).
[21] J. D. Reuss, M. Vlad, and J. H. Misguich, Phys. Lett. A **241**, 94 (1998).
[22] M. Vlad, F. Spineanu, J. H. Misguich, and R. Balescu, Phys. Rev. E **58**, 7359 (1998).
[23] A. V. Gruzinov, M. B. Isichenko, and Y. L. Kalda, Sov. Phys. JETP **70**, 263 (1990).
[24] M. B. Isichenko, Rev. Mod. Phys. **64**, 961 (1992).
[25] T. Hauff and F. Jenko, Phys. Plasmas **14**, 092301 (2007).
[26] J. Wesson, *Tokamaks* (Clarendon, Oxford, 1987), Chap. 3.
[27] T. Hauff and F. Jenko, Phys. Plasmas **13**, 102309 (2006).